IOP Conf. Series: Journal of Physics: Conf. Series **820** (2017) 012018 doi:10.1088/1742-6596/820/1/012018

The Synthesis and Characterization of $Ag/Ag_2O/TiO_2$/NGP Composites as Adsorbents and Photocatalysts for Wastewater Removal

A. Taufik[1,2], S.P. Prakoso[2], R. Saleh[1,2,a]
[1]Departemen Fisika, Fakultas MIPA-Universitas Indonesia, 16424 Depok, Indonesia

[2]Integrated Laboratory of Energy and Environment, Fakultas MIPA-Universitas Indonesia, 16424 Depok, Indonesia

[a]Corresponding's author: rosari.saleh@gmail.com, rosari.saleh@ui.ac.id

Abstract. An $Ag/Ag_2O/TiO_2$/NGP with different nanographene platelets (NGP) weight percents was synthesized using the hydrothermal method. The NGP weight percent was 5, 10, and 15 weight percent, respectively. The structural properties of the samples were characterized by X-ray diffraction. The optical properties of the samples were investigated by UV-Vis spectroscopy and their thermal properties were investigated by Thermo Gravimetric Analysis and Differential Thermal Analysis. The existence of a cubic structure from Ag and Ag_2O, an anatase from TiO_2, and a graphitic like structure from NGP indicated that the samples were successfully formed. The maximum light absorption at 435 nm indicated the existence of surface plasmon resonance (SPR) from silver nanoparticles. The phase transformation of Ag_2O to Ag occurred at 435 °C. Adsorption and the photocatalytic performance were investigated in the degradation of methylene blue from the aqueous solution. The adsorption ability of $Ag/Ag_2O/TiO_2$/NGP composites increased by increasing the NGP weight percent. The adsorption process of MB followed pseudo-second-order kinetic reactions. The photocatalytic activity of $Ag/Ag_2O/TiO_2$/NGP showed that $Ag/Ag_2O/TiO_2$/NGP with a 10 weight percent NGP exhibited the highest photocatalytic performance, with a removal ability of approximately 96 percent.

1. Introduction

Recently, organic dyes have been widely used in many fields, such as the textile, rubber, paper, and printing industries [1]. However, the wide range of applications of organic dyes caused environmental problems due to their hazardous properties. A portion of used organic dyes is discharged into the natural environment via industrial wastewaters, posing severe threats to aquatic organisms and human health due to the high toxicity and low biodegradability of synthetic organic dyes [2-4]. Therefore, it is important to treat organic dyes in industrial waste before they are discharged into the environment. Adsorption has been widely used in wastewater treatment due to its simple design, low-cost, and easy operation [5].

Many adsorbent materials, such as zeolite, clay, activated carbon, and graphene, have been used to remove organic dye from the environment. [6]. Graphene has been considered to be a promising material as an adsorbent due to its high specific surface area, high adsorption capacities, rapid adsorption rates, and tunable functionality of surface properties along with the intriguing mechanical, thermal, and electrical properties of the constitutive materials [6]. However, adsorption techniques merely transfer dye pollutants from one phase to another, and the pollutants are not degraded well or removed [7]. Therefore, it is very important to find an effective method to enhance the removal of organic dyes.

Photocatalytic technology is a desirable method for energy generation and wastewater treatment, because it is an inexpensive and convenient, and can completely decompose dye molecules into inorganic small molecules [8]. Numerous studies have addressed the photocatalytic performance of an oxide semiconductor [8]. TiO_2 has been considered as a photocatalyst over past two decades due to its high photocatalytic performance, high chemical and thermal stability and it was inexpensive [9]. However, TiO_2 still has several drawbacks, such as a high-rate recombination electron and holes, and it could be activated only under UV light irradiation due to its wide bandgap (3.2 eV) [9,10]. Several studies reported that many methods could improve the photocatalytic performance of a catalyst; methods included the deposition of noble metal, such as silver, coupled with a narrow bandgap semiconductor, such as Ag_2O [10,11].

Based on the aforementioned explanation, this research evaluates the comparison between adsorption and the photocatalytic performance of a combination of TiO_2, graphene, Ag, and Ag_2O in $Ag/Ag_2O/TiO_2$/nanographene platelets (NGP) composites. The structural, thermal, and optical properties of the samples were investigated to confirm the existence of $Ag/Ag_2O/TiO_2$/NGP. This study will investigate the adsorption ability of the samples, the kinetic study and photocatalytic mechanism.

2. Experimental

2.1. Synthesis $Ag/Ag_2O/TiO_2$/NGP

All reagents used were analytical grade and had no further purifications. Ag/Ag_2O/TiO2/NGP with different NGP weight percent were synthesized using microwave assisted method. Typically, $AgNO_3$ (silver nitrate), TiO_2, and nanographene were dispersed in 40 mL DI water using magnetic stirrer. Then, 80 mL SDS (sodium dodecyl sulfate) was added into the above solution. After that, 10 mM of NaOH were added into the solution and stirred for 10 min. After the homogeneous solution was achieved, the solution was irradiated by a microwave wave operated at 800 W for 2 min. The solution was then centrifuged and washed using ethanol and DI water to remove the unnecessary substances. The precipitated was dried under air condition at 120 °C for 5 hours. The NGP amounts were 5, 10, and 15 weight percent, respectively, on the $Ag/Ag_2O/TiO_2$ nanocomposites.

2.2. Characterization

The structural properties of the samples were characterized by an X-ray diffraction (XRD) Rigaku Miniflex 600 operated at 30 kV and 15 mA and monitored in the range 2θ =10° - 90°. The optical properties of the samples were investigated by a UV-Vis spectrometer Hitachi UH5300 from 200 nm to 800 nm. The thermal properties of the samples were investigated using DTA/TGA (Rigaku Thermo Plus EVO2 TG-8121), with alumina as a reference and operated at room temperature until 500 °C.

2.3. Adsorption and Photocatalytic measurement

Adsorption and the photocatalytic performance of $Ag/Ag_2O/TiO_2$/NGP were tested on the degradation of methylene blue (MB) from the aqueous solution. Typically, 20 mg/L of MB were poured into a 100 mL beaker glass. After that, 0.03 g of $Ag/Ag_2O/TiO_2$/NGP were added to the solution and kept in the dark for 4 hours. At the specified time interval, the methylene blue solution was collected and monitored by UV-Vis spectroscopy to investigate the degradation of methylene blue. Its degradation was calculated using the following equation:

$$Degradation: \frac{C_t}{C_0}, \quad \text{(eq.1)}$$

where C_0 was the initial dye concentraton and C_t was the dye concentration after time t. The absorption capacity of $Ag/Ag_2O/TiO_2$/NGP composites was calculated using:

$$q_e = \frac{(C_o - C_e)V}{m}, \quad \text{(eq.2)}$$

where q_e represents the equilibrium adsorption capacity of the Fe_3O_4 nanocomposite (mg/g); C_0 and C_e are the initial and equilibrium concentrations of methylene blue (mg/L) in aqueous solutions, respectively; V is the volume of the aqueous MB (mL); and m is the amount of $Ag/Ag_2O/TiO_2$/NGP used (g). After 4-hour adsorption process, the solution was irradiated using a 40 W Xe lamp for 2 hours, and every 15 minutes, the MB solution was taken and monitored by UV-vis spectroscopy to investigate the degradation process.

3. Result and Discussion

Figure 1 shows the XRD spectra of $Ag/Ag_2O/TiO_2/NGP$ with different NGP weight percents. The comparison the XRD spectra of $Ag/Ag_2O/TiO_2$, without the addition of NGP, was also plotted in the figure. The XRD result from $Ag/Ag_2O/TiO_2/NGP$ revealed several diffraction patterns that corresponded to the existence of a cubic structure from Ag_2O and Ag nanoparticles, an anatase structure from TiO_2, and a graphiticlike structure from NGP materials. The result showed that the diffraction pattern at 2θ = 26° increases with an increase in the NGP weight percent. It indicated the higher NGP loading on the samples. The lattice parameter and grain size of the samples were

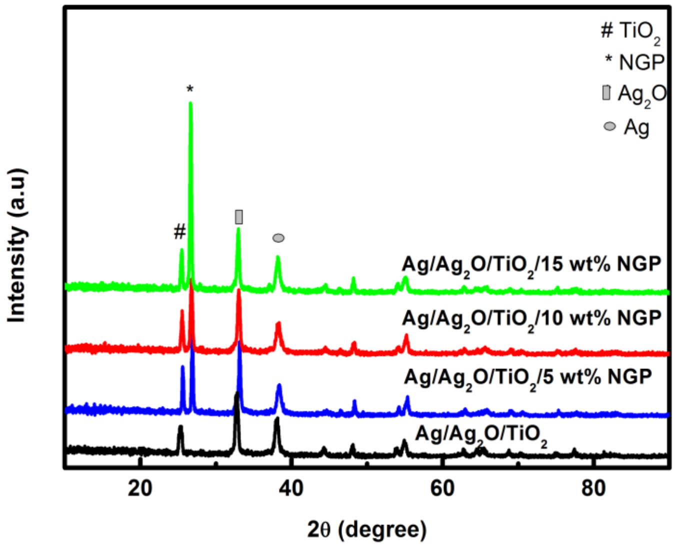

Figure 1. XRD spectra of $Ag/Ag_2O/TiO_2/NGP$ with different NGP weight percent. Black (0 wt%), blue (5 wt%), red (10 wt%), green (15 wt%).

Table 1. Lattice parameter and grain size of $Ag/Ag_2O/TiO_2/NGP$ with different NGP weight percent.

	Lattice Parameter					Grain size (nm)			
	Ag	Ag_2O	TiO_2		NGP				
Sample	a=b=c	a=b=c	a=b	c	a=b=c	Ag	Ag_2O	TiO_2	NGP
$Ag/Ag_2O/TiO_2$	4.094	4.736	3.791	9.529	-	20	19	31	-
$Ag/Ag_2O/TiO_2$/5 wt% NGP	4.072	4.683	3.747	9.277	3.600	13	36	37	32
$Ag/Ag_2O/TiO_2$/10 wt% NGP	4.070	4.696	3.749	9.469	3.491	13	27	32	33
$Ag/Ag_2O/TiO_2$/15 wt% NGP	4.068	4.706	3.762	9.455	3.627	16	23	31	33

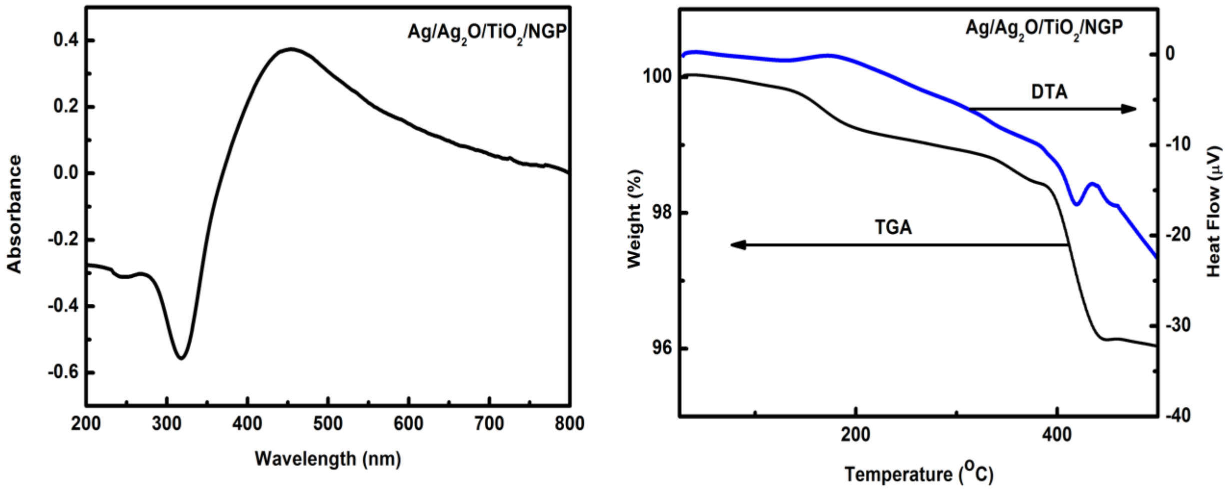

(a) (b)

Figure 2. (a) UV-Vis absorbance and (b) DTA/TGA measurement of $Ag/Ag_2O/TiO_2$/NGP composites.

calculated using the Retveld Refinement method and Debye-Scherer Equation, respectively. The lattice parameter and grain size of the corresponding materials in $Ag/Ag_2O/TiO_2$/NGP composites are tabulated in Table 1. The table shows that the corresponding lattice parameter from Ag, Ag_2O, TiO_2, and NGP materials does not change significantly. It indicates that the all prepared samples have the same structural properties. It could be observed from the XRD result that the incorporation of NGP could enhance the Ag loading on the samples. The figure shows a diffraction peak at $2\theta = 38°$ that corresponds to the cubic structure from a silver increase with increased NGP loading.

To understand the behavior of silver nanoparticles, the optical properties of $Ag/Ag_2O/TiO_2$/NGP composites were measured (Figure 2(a)). The figures show that the prepared sample has broad light absorption, with the maximum absorbance intensity of 435 nm. Rather et al. reported that the absorbance behavior corresponded to the existence of Surface Plasmon Resonance (SPR) from silver nanoparticles [12].

The thermal properties of the samples were characterized by the DTA/TGA measurement, and the results are shown in Figure 2(b). The DTA/TGA measurement of $Ag/Ag_2O/TiO_2$ nanocomposites revealed several weight losses, such as at 100 °C to 200 °C, that corresponded to the removal of the absorbed water from the samples. The significant weight lost from $Ag/Ag_2O/TiO_2$ occurs at 400 °C to 437 °C due to the phase transformation from Ag_2O into Ag nanoparticles [13]. The DTA measurement of $Ag/Ag_2O/TiO_2$ showed that the transformation of Ag_2O into Ag nanoparticles was an exothermic

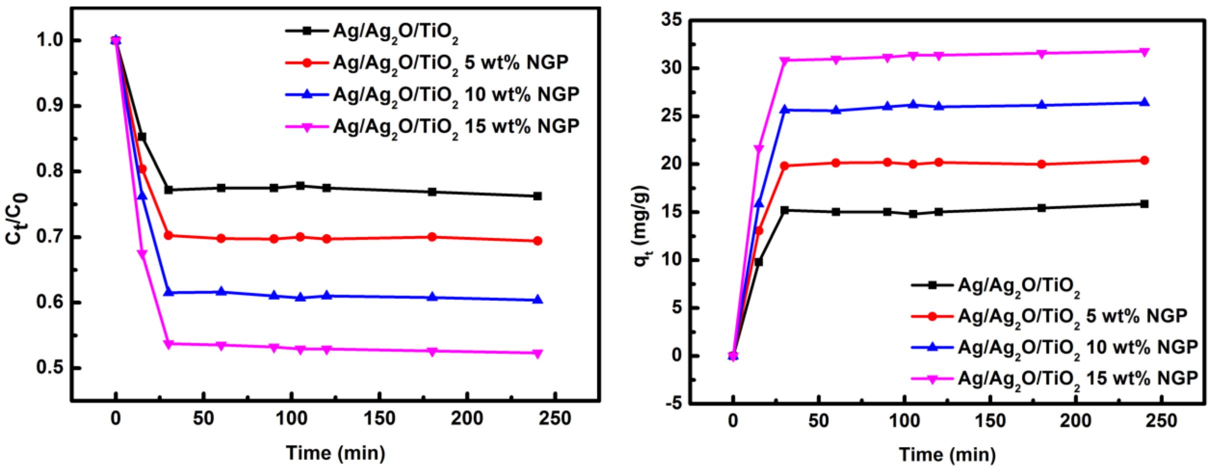

(a) (b)

Figure 3. (a) Decolorization of NGP using $Ag/Ag_2O/TiO_2$/NGP composites through adsorption process. (b)Adsorption capacity of $Ag/Ag_2O/TiO_2$/NGP composites.

process.

Figure 3(a) shows the decolorization of MB after an absorption process that uses $Ag/Ag_2O/TiO_2$/NGP composites with different NGP weight percents. The result shows that the absorption ability of $Ag/Ag_2O/TiO_2$ nanocomposites increases with the incorporation of NGP materials. Higher NGP loading also resulted in a higher absorption ability. Samples with higher NGP loading exhibit the highest absorbance ability. Figure 3(b) shows the adsorption capacity of all prepared samples. As can be seen from the figure that the adsorption capacity of $Ag/Ag_2O/TiO_2$/NGP increase with increasing NGP weight percent. It indicates that NGP materials are very important in the absorption ability of the samples.

The kinetic model of the adsorption process was investigated using pseudo-first-order and second-order kinetic reactions [14]: The derivation of pseudo first-order-kinetic reactions is given by the following equations:

$$q_t = q_e(1 - \exp(-K_1 t)) \quad \text{(eq.3)}$$
$$q_t = q_e - q_e \exp(-K_1 t) \quad \text{(eq.4)}$$
$$\ln q_t = \ln q_e - \ln(q_e \exp(-K_1 t)) \quad \text{(eq.5)}$$
$$\ln q_t = \ln q_e - (\ln q_e + (-K_1 t)) \quad \text{(eq.6)}$$
$$\ln(q_e - q_t) = \ln q_e - K_1 t \quad \text{(eq.7)}$$

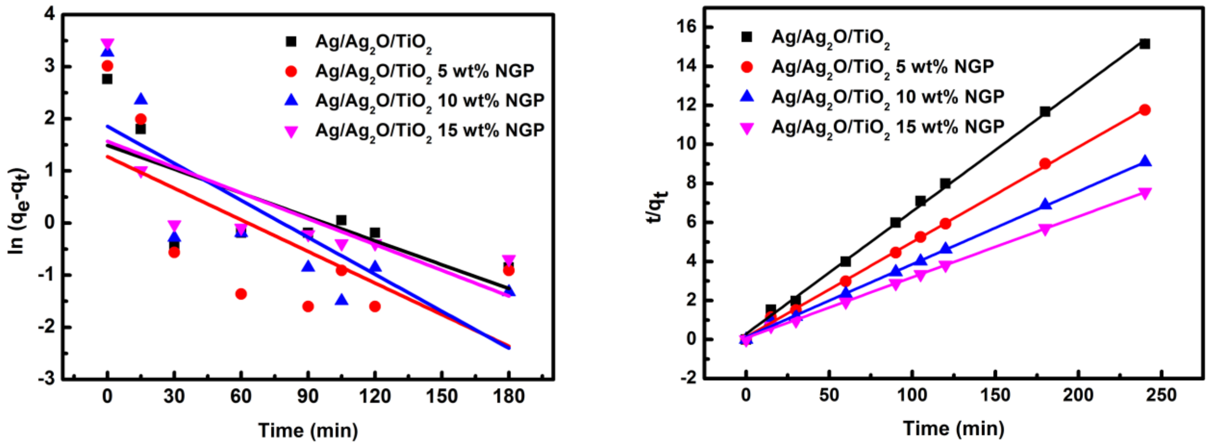

(a) (b)

Figure 4. (a) Pseudo first and (b) second order kinetic reactions model.

Table 2. Fitting result from pseudo first and second order kinetic reactions.

Sample	qe (mg/g) exp	The pseudo-First-order rate qe (mg/g) cal	K_1	R^2	The pseudo-second-order rate qe (mg/g) cal	K_2	R^2
$Ag/Ag_2O/TiO_2$	15.85	1.91	0.00660	0.47	15.93	0.013406	0.99
$Ag/Ag_2O/TiO_2$/5 wt% NGP	20.38	1.74	0.00877	0.40	20.54	0.018022	0.99
$Ag/Ag_2O/TiO_2$/10 wt% NGP	26.41	2.24	0.01027	0.60	26.78	0.010835	0.99
$Ag/Ag_2O/TiO_2$/15 wt% NGP	31.78	2.44	0.01076	0.68	32.11	0.011616	0.99

while the pseudo second order kinetic reactions were derived by:

$$q_t = \frac{q_e^2 K_2 t}{1+q_e K_2 t} \quad \text{(eq.9)}$$

$$\frac{1}{q_t} = \frac{1+q_e K_2 t}{q_e^2 K_2 t} \quad \text{(eq.10)}$$

$$\frac{1}{q_t} = \frac{1}{q_e^2 K_2 t} + \frac{q_e K_2 t}{q_e^2 K_2 t}\ multiple\ by\ t \quad \text{(eq.11)}$$

$$\frac{t}{q_t} = \frac{1}{q_e^2 K_2} + \frac{t}{q_e} \quad \text{(eq.12)}$$

q_e and q_t are the adsorption capacities at equilibrium and time t, respectively. K_1 is the pseudo-first-order kinetic constant (min^{-1}), and K_2 is the pseudo-second-order constant (g/(mg min)). The pseudo-first-order and pseudo-second-order models are plotted in Figures 4(a) and (b), respectively. The fitting parameters are given in Table 2. It can be seen from the tables that the fitting experimental data is more fitted with pseudo-second-order kinetic reactions than pseudo-first-order kinetic reactions.

The photocatalytic activity of all samples is shown in Figure 5. The figures show that the incorporation of NGP could enhance the photocatalytic activity. The degradation percentage of all samples is tabulated in Table 3. The degradation efficiency increase from 76% to 95% with increasing NGP from 0, 5, until 10 wt% NGP. The enhancement of photocatalytic performance $Ag/Ag_2O/TiO_2$/NGP compare tp $Ag/Ag_2O/TiO_2$ is due to the existence of NGP could prevent recombination electron and holes and therefore enhance the photocatalytic efficiency. However, the increasing NGP loading until 15 wt% the photocatalytic activity of $Ag/Ag_2O/TiO_2$/NGP decrease. It is probably because the higher NGP loading could have prevented the light from penetrating the samples.

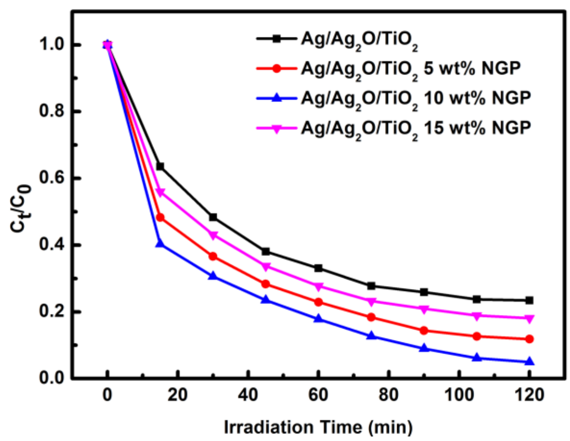

Figure 5. Photocatalytic activity of $Ag/Ag_2O/TiO_2$/NGP with different NGP weight percent.

Table 3. Percentage degradation of photocatalytic activity of $Ag/Ag_2O/TiO_2$/NGP with different NGP weight percent.

Sample	Photocatalytic degradation (%)
$Ag/Ag_2O/TiO_2$	76
$Ag/Ag_2O/TiO_2$/5 wt% NGP	88
$Ag/Ag_2O/TiO_2$/10 wt% NGP	95
$Ag/Ag_2O/TiO_2$/15 wt% NGP	82

4. Conclusion

$Ag/Ag_2O/TiO_2$/NGP composites with different NGP weight percents were successfully synthesized using the hydrothermal method. The existence of silver nanoparticles induced the surface plasmon resonance to improve the charge separation process in photocatalytic activity. The incorporation of NGP could enhance the adsorption ability and photocatalytic performance for remove organic dye from the aqueous solution. The higher NGP loading from 5, 10, and 15 wt% in $Ag/Ag_2O/TiO_2$/NGP composites resulted in higher adsorption performance and the photocatalytic performance of $Ag/Ag_2O/TiO_2$/NGP composites with 10 wt% NGP resulted in higher photocatalytic performance. The adsorption performance of $Ag/Ag_2O/TiO_2$/NGP composites followed pseudo-second-order kinetic reaction.

Reference

[1] F. Zhang, X. Chen, F. Wu, Y. Ji 2016 *Colloids Surf.,* ***509*** 474–483.
[2] Y. Qi, M. Yang, W. Xu, S. He, Y. Men 2017 *J. Colloid Interface Sci.* **486** 84–96.
[3] L. Liu, Z.Y. Gao, X.P. Su, X. Chen, L. Jiang, J.M. Yao 2015 *ACS Sustain. Chem. Eng.* **3** 432–442.
[4] G. Crini 2006 *Bioresour. Technol.* **97** 1061–1085.
[5] S. Yang, Y. Wu, Y. Wu, L. Zhu 2015 *J. Taiwan Inst. Chem. E* **50** 205–214.
[6] H. Kim, S.O. Kang, S. Park, H.S. Park 2015 *Ind. Eng. Chem. Res.* **21** 1191–1196.
[7] P. Nuengmatcha, S. Chanthai, R. Mahachai, W.C. Oh 2016 *Journal of Environmental Chemical Engineering* **4** 2170–2177.
[8] G. Hai, J. Huang, L. Cao, Y. Jie, J. Li, X. Wang, G. Zhang 2017 *J. Alloys Compd.* **690** 239–248.
[9] L. Liu, C. Luo, J. Xiong, Z. Yang, Y. Zhang, Y. Cai, H. Gu 2017 *J. Alloys Compd.* **690** 771–776.
[10] N. Wei, H. Cui, Q. Song, L. Zhang, X. Song, K Wang, Y. Zhang, J. Li, J. Wen, J. Tian 2016 Appl. Catal., B **198** 83–90.
[11] Y.C Yao, X.R. Dai, X.Y. Hu, S.Z. Huang, Z. Jin 2016 *Appl. Surf. Sci.* **387** 469–476.
[12] R.A. Rather, S. Singh, B. Pal 2017 *Sol. Energy Mater. Sol. Cells* **160** 463–469.
[13] A. Sakulkalavek, R. Sakdanuphab 2016 *Mater. Sci. Semicond. Process.* **56** 313–323.
[14] A.N.M. Salem, M.A. Ahmed, M.F.E. Shahat 2016 *J. Mol. Liq.* **219** 780–788.